Observation of the Component Dynamics in a Miscible Polymer Blend by Dielectric and Mechanical Spectroscopies

A. Alegría and J. Colmenero

Departamento de Fisica de Materials, Universidad del Pais Vasco (UPV/EHU), Facultad de Quimica, Apartado 1072, 20080 San Sebastian, Spain

K. L. Ngai* and C. M. Roland

Naval Research Laboratory, Washington, D.C. 20375-5000

Received January 18, 1994; Revised Manuscript Received May 17, 1994[⊕]

ABSTRACT: Dielectric and mechanical relaxation measurements of the local segmental relaxation in miscible blends of poly(vinylethylene) (PVE) and polyisoprene (PIP) have been made under isothermal conditions over a wide range of frequency. Taking advantage of the prominence of respectively the PVE contribution to dielectric relaxation and the PIP contribution to mechanical relaxation, we are able to resolve the dynamics of each component in some of the blends. From the observed dynamics of individual components, we establish as experimental facts that the most probable local segmental relaxation time of each component has a different magnitude as well as different temperature dependence. Moreover, the relaxation spectrum of each component broadens as temperature is decreased. Thus a breakdown of thermorheological simplicity occurs not only in the dynamics of each component but a fortiori when the contributions from both components are considered together. The degree to which these effects manifest themselves depends on the blend composition. All these experimental features are shown to be in accord with a theory of segmental dynamics for blends that is obtained as a generalization of the coupling model for homopolymers by taking into account local concentration fluctuations.

Introduction

Polymer blends not only have practical value in diverse applications but also are of great interest in the study of viscoelasticity. The viscoelastic behavior of miscible polymer blends can be quite different from that of homopolymers. These differences are seen in the local segmental relaxation responsible for the glass transition as well as in the terminal relaxation region. In this paper we shall confine our attention to local segmental relaxation, which in blends is often associated with anomalously broad glass transitions[1-6] and a breakdown of time–temperature superposition.[7-10] The origin of these remarkable properties of blends have been traced[7-10] to the occurrence of distinct mobilities for each component of the binary blend. The different dynamics of the two kinds of chains are appropriately described as "dynamical heterogeneity". ^{13}C NMR,[6] mechanical,[7,13] dielectric,[3,9,10,12,13] dynamic light scattering,[13] and deuteron NMR[11] measurements in the glass transition region of miscible blends have provided detailed information on the nature of the dynamical heterogeneity.

Within a miscible blend the local composition is known to fluctuate about its average value. These concentration fluctuations give rise to a distribution of local compositions. Concentration fluctuations have previously been identified as a mechanism for broadening of the relaxation spectra in the glass transition region.[7,15] Two recent theoretical models,[8,14] proposed to describe dynamical heterogeneity in blends, are both based on a distribution of local composition. One example is the model of Ngai and Roland,[8,10,12,15] which is a generalization of the coupling model for homopolymers to binary blends. Dynamic mechanical[8] and dielectric relaxation,[9,10,12] measurements of the glass transition region for miscible blends have been analyzed and the results interpreted successfully in terms of the model. Among these studies are dynamic mechanical measurements of 1,4-polyisoprene and poly(vinylethylene) blends. Both components contribute to the mechanical modulus, although the individual contributions cannot be clearly resolved. For equal weights of the two components, PIP contributes more prominently to the loss modulus of the blend, due in part to the higher and narrower loss modulus peak of pure PIP as compared with that of pure PVE. As a consequence, the location of the maximum of the loss modulus corresponds more closely to that of PIP, particularly in blends of lower PVE content. In spite of the difficulty of resolving the contributions of the two components, fitting the mechanical data of the blends to the theoretical model[8] enabled the respective dynamics of the two components to be determined. The separate contributions to the loss modulus from the components can be calculated from the parameters determined in ref 8.

In this work similar blends are studied both dielectrically and mechanically over a wide range of temperatures. As shown by neutron scattering, this blend is miscible over all the composition range and all experimentally accessible temperatures.[16] The dielectric strength of PVE is larger than that of PIP (by about a factor of 2), making the former's contribution to the dielectric loss more prominent. This situation is to be contrasted with the mechanical loss modulus in which the reverse (i.e., stronger PIP contribution) is the case. In blends of lower PVE content, the interplay of dielectric strength and concentration of PVE gives rise to the possibility that in some composition range the respective dielectric loss peaks for the two components can be resolved. Thus, the present study should be an interesting complement to previous ones which relied on a single experimental technique. The results provide precise information on the dynamics of the individual components, allowing comparisons to predictions previously drawn from the theoretical model.

Experimental Section

The PVE and PIP blends used herein for dielectric and mechanical relaxation measurements are similar to those studied earlier by dynamic mechanical spectroscopy.[8] However, since

[⊕] Abstract published in *Advance ACS Abstracts*, June 15, 1994.

0024-9297/94/2227-4486$04.50/0

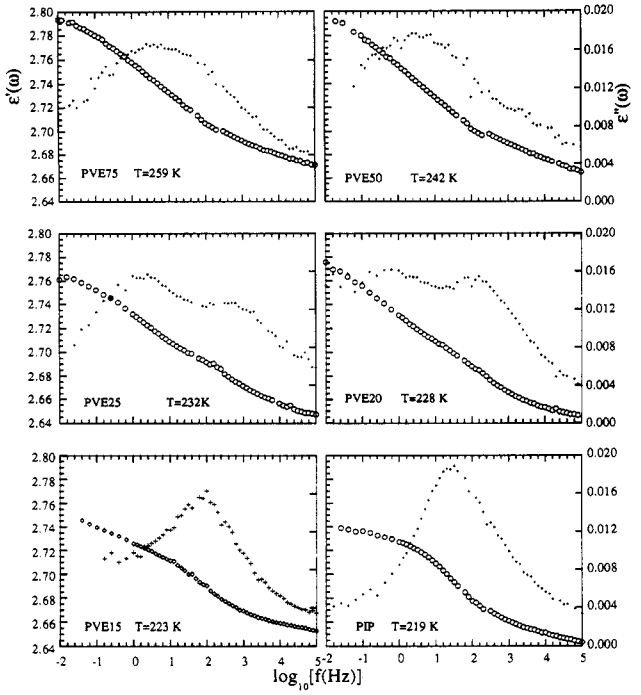

Figure 1. Real and imaginary parts of the dielectric susceptibility at constant temperatures for pure PIP and five blends.

the earlier experiments relied on a tensile geometry, those materials were lightly cross-linked to minimize creep. Although the effect of cross-linking is minified for measurements carried out near the glass transition zone, there is a systematic increase with cross-link density of both the relaxation time and breadth of the segmental relaxation peak.[17] We avoid this complication herein by using un-cross-linked materials with a torsional geometry. The poly(vinylethylene) was 97% 1,2-polybutadiene obtained from the Firestone Tire and Rubber Co. The *cis*-1,4-polyisoprene was a high purity grade of *Hevea brasiliensis* (SMR-L from the Ore and Chemical Corp.). The latter was dissolved and filtered to remove small traces of naturally occurring gel. Five blends, designated PVE-75, PVE-50, PVE-25, PVE-20, and PVE-15, where the number denotes the percentage by weight of the poly(vinylethylene), were studied.

The dynamic mechanical data were obtained with a Bohlin VOR rheometer using 6 mm diameter parallel plates with typically a 0.8 mm gap. Isothermal data were obtained at various temperatures in the vicinity of T_g at frequencies between 10^{-4} and 10^{1} Hz.

Dielectric relaxation measurements was conducted with a BS4000 system from Novocontrol GmbH. This system includes a Solartron-Schumberger gain/phase analyzer SI1260 and a high input impedance buffer amplifier Chelsea Dielectric Interface. The frequency range covered was from 10^{-2} to 10^{5} Hz. The experimental limit for the loss factor was about 10^{-4}. The sample was kept between gold-plated stainless steel electrodes of a parallel plate capacitor. The frequency scans were performed isothermally following decreasing temperature steps, with the sample temperature maintained constant to within ±0.02 K.

Results

Figure 1 shows both the real and imaginary parts of the dielectric susceptibility, ϵ'', as functions of frequency at constant temperatures for pure PIP and five different blends. The PIP sample used in the experiments has a high molecular weight and broad molecular weight distribution. As a consequence the normal mode relaxation,[18,19] located many decades of frequency below the segmental relaxation, does not appear or contribute within our experimental window. Starting from pure PIP (PVE-0) and going to PVE-15, the dielectric loss exhibits only one peak (Figures 2 and 3). Although in PVE-15 there is significant contribution from conductivity relaxation at

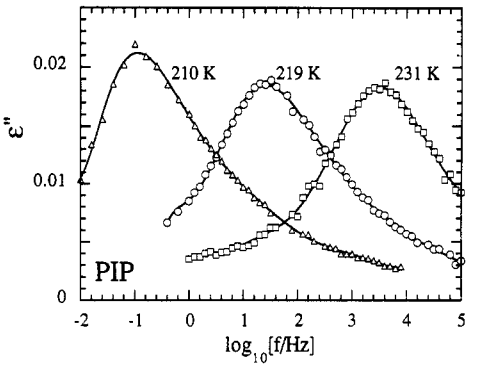

Figure 2. Frequency dependence of dielectric loss at various temperatures for PIP. For clarity only data taken at several representative temperatures are shown here.

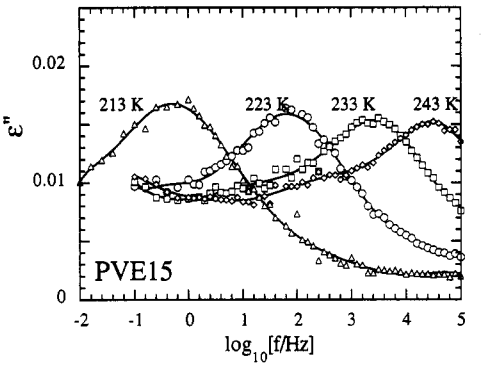

Figure 3. Frequency dependence of dielectric loss at various temperatures for PVE-15 blend. For clarity only data taken at several representative temperatures are shown here.

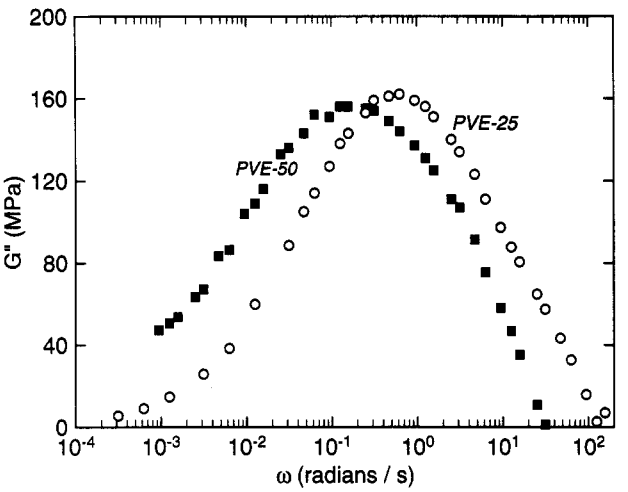

Figure 4. Shear loss modulus spectra at a temperature of −60 °C for PVE-25 blend and at a temperature of −57 °C for PVE-50.

low frequencies, there is still clear evidence that the peak is broadened on the low frequency side in the presence of 15% PVE. The central peak structure presumably originates from the majority PIP component. The broadening to low frequencies has not been seen before in dynamical mechanical relaxation measurements in blends with low PVE content. In fact dynamic mechanical loss data of a previous set of blends[8] and the present ones do not show such a low frequency tail. In the blends with less than 50% PVE, the dynamical mechanical loss peaks are nearly symmetric in shape (see Figures 4 and 5). The difference between the results from the two spectroscopies is a consequence of the dominance of respectively the contribution from the PVE component in dielectric loss and the contribution from the PIP component in dynamic mechanical loss (see Figure 6, which compares the

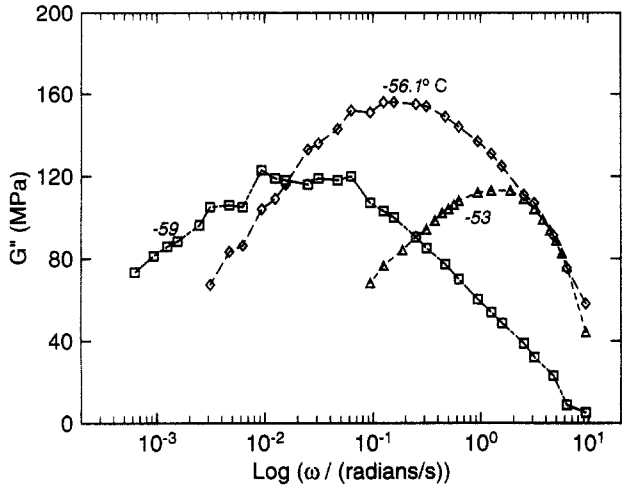

Figure 5. Variation of the shear loss modulus spectrum with temperature for PVE-50 blend showing the breakdown of thermorheological simplicity. The triangles, diamonds, and squares stand for data points taken at the three temperatures indicated. The lines are guides for the eye.

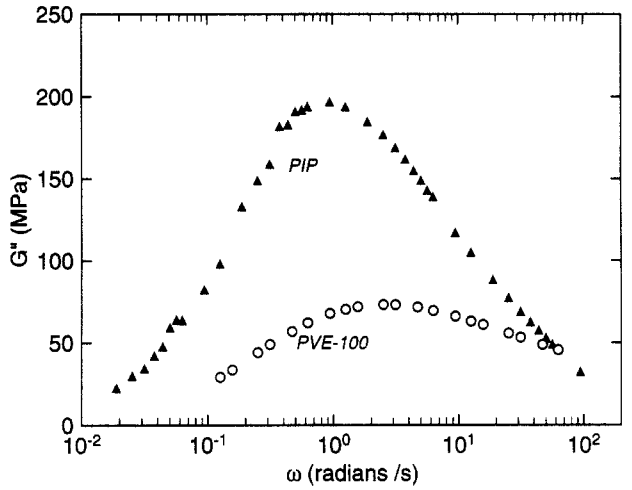

Figure 6. Comparison of the mechanical shear loss spectrum of pure PIP at T = −64 °C and of pure PVE at T = −4 °C.

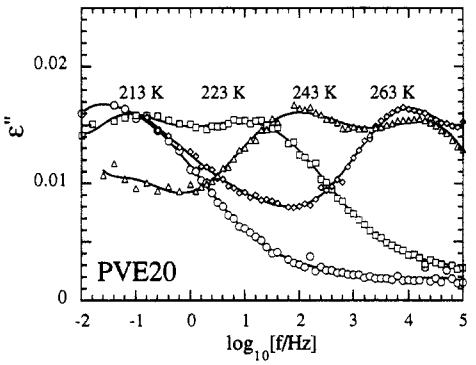

Figure 7. Frequency dependence of dielectric loss at various temperatures for PVE-20 blend. For clarity only data taken at several representative temperatures are shown here.

mechanical loss of pure PIP with that of pure PVE). This interpretation is confirmed by dielectric data of PVE-20 (Figure 7) in which an additional peak now appears at lower frequencies, and of PVE-25 (Figure 8) in which this new peak has increased in height to become the more dominant. This trend in the measured spectra leaves little doubt that the lower frequency dielectric loss peak is related to the PVE component and the higher frequency peak to the PIP component. Whence for the case of the two PVE-x blends with x = 20 and 25, in which two

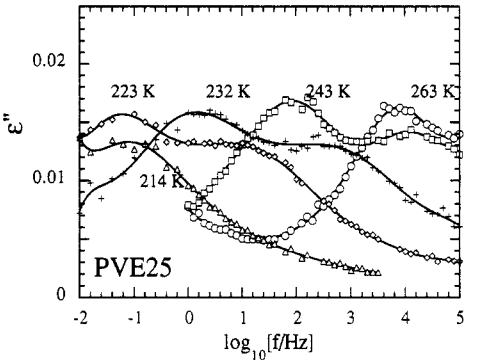

Figure 8. Frequency dependence of dielectric loss at various temperatures for PVE-25. For clarity only data taken at several representative temperatures are shown.

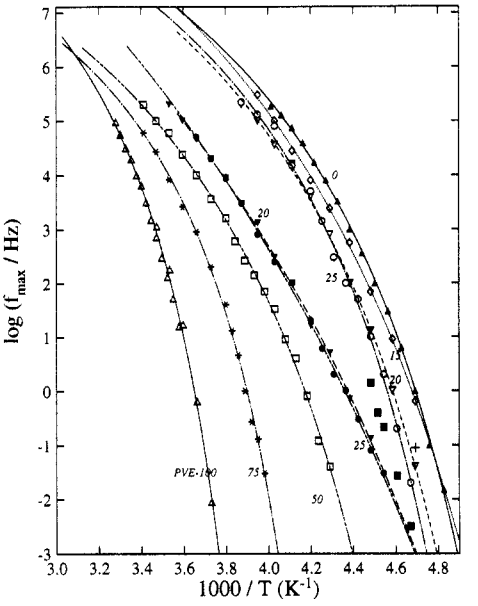

Figure 9. log (frequency) against reciprocal temperature for mechanical (shear modulus loss maximum, filled solid squares for PVE-50, crosses for PVE-25) and dielectric loss maximum (all other symbols) for PVE/PIP blends, near PIP, and neat PVE. Continuous curves are Vogel–Fulcher fits to the experimental points. The PVE content is as indicated. In two blends, for which two dielectric loss maxima were observed, the higher frequency loss maximum is represented by the open inverted triangle (x = 20) and the open circle (x = 25), and the lower frequency loss maximum is represented by the filled inverted triangle (x = 20) and the filled circle (x = 25).

dielectric loss peaks appear, we shall denote the frequency of the lower frequency peak by f_{dPVE} and the frequency of the higher frequency peak by f_{dPIP}. These quantities are plotted as a function of reciprocal temperature for the two blends in Figure 9. In this plot we also show the corresponding data for PVE-0 and PVE-15, in which there is only one peak. The continuous curves are Vogel–Fulcher fits to the temperature dependencies of f_{dPVE} and f_{dPIP} of the blends. The Vogel–Fulcher parameters are given in Table 1.

In contrast to dielectric measurements, dynamical mechanical data in all the blends studied do not show two resolved peaks. The frequency of the lone dynamic mechanical loss peak, f_m, determined for the PVE-25 blend from data shown in Figure 4 at a single temperature is also displayed in Figure 9. For the PVE-25 blend a comparison of f_m with f_{dPIP} and f_{dPVE} shows that f_m lies much closer to f_{dPIP} than to f_{dPVE} at the same temperature. This close correspondence between the mechanical loss peak and the dielectric loss peak of the PIP component confirms the

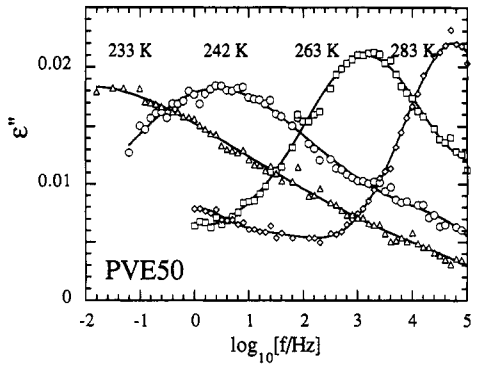

Figure 10. Frequency dependence of dielectric loss at various temperatures for PVE-50. For clarity only data taken at several representative temperatures are shown.

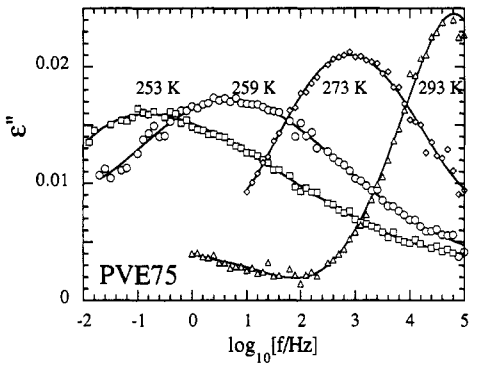

Figure 11. Frequency dependence of dielectric loss at various temperatures for PVE-75. For clarity only data taken at several representative temperatures are shown.

Table 1. Parameters Used in Fitting the Vogel–Fulcher Equation, $\log \tau^* = A + B/(T - T_0)$, to the Dielectric Data

	A (s)	B (K)	T_0 (K)
PIP	5.50×10^{-13}	1.09×10^3	171.8
PVE-15	1.25×10^{-14}	1.68×10^3	158.2
PVE-20 (peak 1)	4.01×10^{-13}	1.23×10^3	172.1
PVE-20 (peak 2)	9.88×10^{-16}	2.97×10^3	138.1
PVE-25 (peak 1)	6.19×10^{-13}	1.09×10^3	178.0
PVE-25 (peak 2)	6.39×10^{-17}	3.52×10^3	130.1
PVE-50	2.30×10^{-12}	1.41×10^3	183.2
PVE-75	1.98×10^{-11}	8.99×10^2	217.1
PVE-100	1.03×10^{-12}	1.02×10^3	234.5

identification of the lone mechanical loss peak of PVE-25 as due mainly to PIP.

On further increase of PVE content (going from PVE-25 to PVE-50 and PVE-75), as shown in Figures 10 and 11 the low frequency PVE dielectric loss peak grows in intensity, overwhelming the contribution from the PIP component. This trend is due to both the higher concentration and the larger dielectric strength of PVE. As a result, the higher frequency PIP loss peak is no longer evident. For these two blends, the frequency of the remaining peak, denoted by f_{dPVE}, is plotted as a function of inverse temperature in Figure 9, along with the fitted Vogel–Fulcher curve. The corresponding data from dynamic mechanical measurements on PVE-50 have been presented in Figure 5. As temperature decreases, the loss modulus peak broadens dramatically. The frequencies of the G'' loss maxima obtained at several temperatures are also plotted in Figure 9. From these data we find that f_m is larger than f_{dPVE} by many orders of magnitude, indicating that even in PVE-50, f_m still corresponds closely to the most probable relaxation frequency of the PIP component.[20]

In PVE-75 the dynamic mechanical loss peak is so broad relative to our experimental frequency range (of about 5 decades) that a peak maximum cannot be unambiguously identified (Figure 12). This is to be contrasted with dielectric loss data of PVE-75, which exhibit a well-defined peak (see Figure 11). However, the $\epsilon''(\omega)$ dispersion broadens rapidly as temperature (or f_m) decreases, which provides an explanation for the enormous breadth of the mechanical loss. The lowest frequency used in dynamic mechanical experiments is about 3 orders of magnitude lower than that available for dielectric relaxation measurements. Despite the difficulty of determining the frequency of the mechanical loss maximum, data at 243 K indicate that f_m is much larger than 10 Hz. Using the Vogel–Fulcher equation for extrapolation, we estimate that at $T = 243$ K the dielectric relaxation peak frequency is about 10^{-5} Hz, or more than 6 decades slower than the mechanical peak. The fact that at 243 K $f_m \gg f_{dPVE}$ evidences the fact that the dynamic mechanical measurements weight heavily the contribution of the PIP component even in PVE-75. Thus, for dynamic mechanical relaxation in all blends with $x \leq 75$ the loss peak frequency f_m can be identified with the characteristic relaxation frequency of the PIP component. In recognition of this, we shall henceforth use the notation f_{mPIP} in lieu of f_m whenever we discuss blends with at least 25% PIP. The dielectric relaxation of pure PVE has previously been measured,[21] and the peak frequency data are plotted in Figure 9.

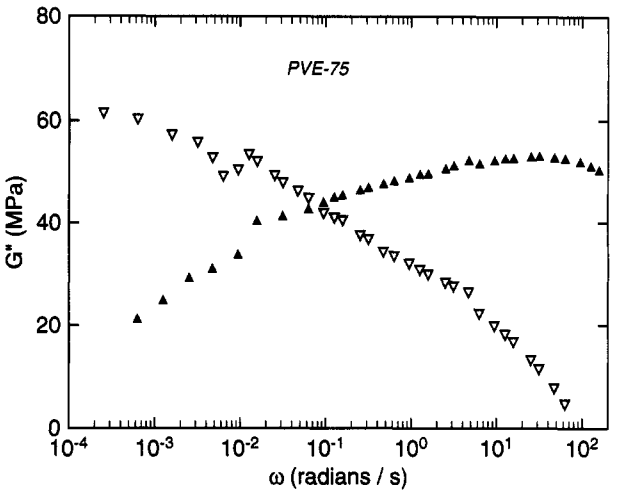

Figure 12. Frequency dependence of shear mechanical loss modulus at $T = -55$ °C (inverted triangles) and at $T = -30$ °C (triangles) for PVE-75.

Coupling Model for Blend Dynamics. In the framework of a generalization of the coupling model to blends[8,10,12,15] each component has its own independent (or primitive) relaxation time, τ_{0i}, $i = 1, 2$, for a binary blend. The distribution of local composition in turn causes a distribution of the local segmental coupling parameter for each component. The local composition has a Gaussian distribution and we assume for convenience that the distribution the coupling parameter has a Gaussian form, $G_i(n_i) = \exp\{-a_i(n_i - \bar{n}_i)^2\}$, in which $\bar{n}_i$ represents the most probable value of the coupling parameter (reflecting the n associated with the average composition) and a_i is a measure of the concentration fluctuation for component i. In principle, an upper and lower cutoff may have to be imposed on the Gaussian distribution to satisfy the bounds on the coupling parameter; in practice, contributions to the calculated spectra become negligible well before this. The dynamics of each component is determined from a heterogeneous superposition of stretched exponentials given by

$$C_i(t) = \int G_i(n_i) \exp(-(t/\tau^*_i(n_i)^{1-n_i})) \, dn_i \quad (1)$$

where

$$\tau^*_i(n_i) = ([1 - n_i]\omega_c^{n_i}\tau_{0i})^{1/(1-n_i)} \quad (2)$$

The proper method for summing the $C_i(t)$ depends on the manner in which the local subvolumes interact mechanically or dielectrically. We can envision two extremes of behavior corresponding to

$$C_{meas}(t) = \sum_i C_i(t) \quad (3)$$

and

$$C^{-1}_{meas} = \sum_i C_i(t)^{-1} \quad (4)$$

From this general formulation several properties of the dynamics of the blend components follow.

(1) Each component has its own most probable relaxation time, $\tau^*_i(\bar{n}_i)$, corresponding to the relaxation of that component in its most probable local composition. Each component has its own distribution width determined by eq 1. The two components, being governed by different dynamics ($\bar{n}_i$, a_i, and τ_{0i}), will have, in general, different temperature dependencies for their most probable relaxation times, $\tau^*_i(\bar{n}_i)$ for $i = 1, 2$.

(2) The heterogeneous distribution of stretched exponential relaxations for *each* component i (eq 1) does not obey time–temperature superposition because of the distribution of coupling parameters, which gives rise to different temperature dependencies of $\tau^*_i(n_i)$. The latter is determined by the shift factor $a_T = [\tau_{0i}(T)/\tau_{0i}(T_0)]^{1/(1-n_i)}$, where T_0 is a reference temperature. It is not difficult to see from eq 2 and this expression for the shift factor that the longer $\tau^*_i(n_i)$'s, corresponding to the larger n_i's within the distribution, will more rapidly shift to longer times as temperature is lowered. The consequence is an asymmetric broadening of the distribution of relaxation rates, resulting at lower temperature in a reversal of the asymmetry associated with neat materials.

(3) The effects described in (2) are manifested to a greater degree for a component with larger $\bar{n}_i$ and a wider distribution $G_i(n_i)$.

(4) The most probable coupling parameter, $\bar{n}_i$, for the ith component in the blend will in general not have the same value as the coupling parameter in the homopolymer. This is an obvious consequence of the change in local composition inherent to blending. In any of the PVE/PIP blends we expect all n_{PVE}'s within the distribution to be less than the coupling parameter, $n_{PVE\text{-}100}$, of PVE homopolymer. This is because from the standpoint of the PVE component, the replacement in any local composition of PVE by the more mobile PIP will mitigate to some extent the dynamic intermolecular constraints. The greater mobility of the PIP is due to its smaller local friction factor (i.e., smaller noncooperative relaxation time, $\tau_{0PIP} \ll \tau_{0PVE}$) and weaker capacity for intermolecular coupling (viz., the value of n for pure PVE is larger than that for neat PIP[18,22,23]). Hence, blending with PIP reduces the value of the coupling parameter for PVE below the homopolymer value. On increasing the PIP content, by the same argument, the mean $\bar{n}_{PVE}$ as well as the entire distribution $\{n_{PVE}\}$ we shift toward lower values.

In blends with sufficiently high PIP content, it is conceivable that $\bar{n}_{PVE}$ may even fall below the PIP homopolymer value. In the coupling model (via eq 2), this falling $\bar{n}_{PVE}$ will have a consequence on the "cooperative plot"[22-26] of log τ_{PVE}* versus $T_{gPVE\text{-}x}/T$, where $T_{gPVE\text{-}x}$ is defined as the temperature at which τ_{PVE}* of the PVE-x blend reaches an arbitrarily chosen but fixed value. As $\bar{n}_{PVE}$ decreases, the steepness of the curve for the PVE component in the blend decreases correspondingly. When $\bar{n}_{PVE}$ falls below the coupling parameter value of homopolymer PIP, we expect the steepness of the curve for the PVE component in the blend to be less than that for homopolymer PIP. This remarkable prediction for the PVE/PIP blend has actually been observed in tetramethyl polycarbonate/polystyrene (TMPC/PS) blends, where TMPC and PS play respectively the roles of PVE and PIP. In an earlier work[12,15] in which the dynamics of the TMPC component could be isolated with dielectric spectroscopy, we have shown that as the TMPC content in the blend decreases, the steepness of the curve for the TMPC component continuously decreases to become less than that of neat PS. We can see whether this prediction, now pertaining to the PVE component, is observed in the PVE/PIP blends.

(5) From the standpoint of the PIP component, blending with PVE replaces PIP with PVE. The latter is less mobile (again in the sense of $\tau_{0PVE} \gg \tau_{0PIP}$) and has more capacity for intermolecular coupling; thus, the intermolecular dynamic constraints experienced by the PIP are enhanced by blending. Its coupling parameter, n_{PIP}, will increase above the neat PIP value. An increase of PVE content in the blend will shift the mean, $\bar{n}_{PIP}$, as well as the entire distribution, $\{n_{PIP}\}$, toward higher values. For a similar reason as discussed above in (4), we expect the steepness of τ_{PIP}* in a cooperativity plot to increase with PVE content in the blend. Such behavior has been seen before in PS/PVME blends where PS and PVME play the role respectively of PVE and PIP herein. Dielectric relaxation measurements on the PS/PVME blends[9] have enabled the dynamics of the PVME component to be selectively monitored. The experimental data verified the expected increase of $\bar{n}_{PVME}$ as well as the steepness of the curve for the PVME component, with increase of PS content. Again we have another opportunity to verify this predicted behavior for PIP in the PVE/PIP blends.

(6) From the trend of n_{PVE} discussed above in (4), we expect the effects described in (2) will be manifested to a much greater degree in PVE-75 than in PVE-25.

Discussion

The results of dielectric and dynamic mechanical measurements on the PVE/PIP blends indicate that from such a combined study the dynamics of each component can be probed. We take advantage of the fact that pure PVE has a larger dielectric strength, such that in blends rich in PIP we can still see the contribution of the PVE. Indeed, in two blends, PVE-20 and PVE-25, the dynamics of the two components have been resolved by dielectric relaxation measurements. In blends with PVE content larger than 25%, dielectric data continue to monitor the PVE dynamics, but the contribution from PVE is so dominant that the PIP component can no longer be resolved. Hence, in PVE-x blends dielectric relaxation spectroscopy alone is sufficient to isolate the PVE dynamics for x in the range $20 \leq x \leq 100$. However, the dynamics of the PIP component can no longer be resolved by dielectric spectroscopy in blends with $x > 25$. Dynamic mechanical relaxation measurements, however, provide information on the PIP dynamics for $25 \leq x \leq 75$.[8] This is the result of the sharper, more intense loss modulus peak of PIP (see Figure 6). Thus, by performing both dielectric and mechanical measurements, we have essentially "resolved" the dynamics of the two components

in the blends. The detailed data for the components provide an opportunity to compare them to the results of various models on the dynamics of blends. The results from the coupling model for miscible blends have been summarized in the previous section. We now enumerate the comparisons between these theoretical results and the experimental data.

(i) Figure 9 shows that in the PVE-20, PVE-25, and PVE-50 blends, *each* component has its own most probable relaxation frequency and temperature dependence. Also from Figures 3 and 8 for PVE-20 and PVE-25, in which relaxations of the two components are resolved by dielectrical measurements, we see two separate distributions of relaxation rates for the components. Each of these distributions is different from that of the corresponding neat polymer. These differences are caused by local composition fluctuations.

(ii) By inspection of the dielectric loss data in Figures 7, 8, 10, and 11 for the PVE-20, PVE-25, PVE-50, and PVE-75 blends, we observe that the dielectric response from the PVE component in any of these blends does not obey time–temperature superposition. The loss peak broadens as the most probable frequency shifts to lower values with decreasing temperature. Upon close examination of the data, we find that the broadening is asymmetric in nature, with the contribution at lower frequency having a larger shift. Similar effects are observed in the dynamic mechanical relaxation data of PVE-50 shown in Figure 5. Of course, the dielectric spectrum of the pure PVE itself does not obey time–temperature superposition,[21] and this is a contributing factor to the blends' thermorheological complexity. However, the degree of thermorheological complexity of neat PVE is relatively small (the full width at half-height of the dielectric loss maximum changes by no more than one decade over a wide temperature range). We conclude that the principal mechanism for failure of time–temperature superposition of the relaxation dynamics of any component in the blend cannot originate from that of the neat material.

(iii) Both the degree of thermorheological complexity and the asymmetry of the broadening increase with PVE content (i.e., going from PVE-20 to PVE-75). Significantly, this is followed by a corresponding increase of the most probable coupling parameter, $\tilde{n}_i$.

(iv) To infer how $\tilde{n}_{PVE}$ varies with blend composition, cooperativity plots of log τ_{PVE}^* vs T_{gPVE-x}/T are constructed (Figure 13). Here τ_{PVE}^* is equal to $1/2\pi f_{dPVE}$ and T_{gPVE-x} has been defined earlier in (4) of the previous section. We use here the convention that $\tau_{PVE}^*(T)$ is equal to 100 s at $T = T_{gPVE-x}$. Shown also in Figure 13 are the cooperativity plots of pure PIP and PVE for comparison with that of the PVE component in the most probable local composition of a blend. The curve for neat PVE is steeper than for pure PIP, consistent with the larger coupling parameter of PVE than PIP.[8] Starting from neat PVE, addition of PIP reduces the steepness (cooperativity) of the curve for the PVE component. The reduction is small in PVE-75, which is understandable in view of PVE being still the majority in this blend. The reduction is quite substantial in PVE-50, with the steepness of the PVE component now falling below that of neat PIP. This trend continues with further addition of PIP. In PVE-25 and PVE-20, Figure 13 shows that the steepness has been substantially reduced from that of pure PIP. This behavior follows exactly the pattern of the TMPC component we have seen before in TMPC/PS blends.[12] An accurate isolation of the contribution from the PVE component in the dielectric loss data of PVE-25 and PVE-20 is difficult,

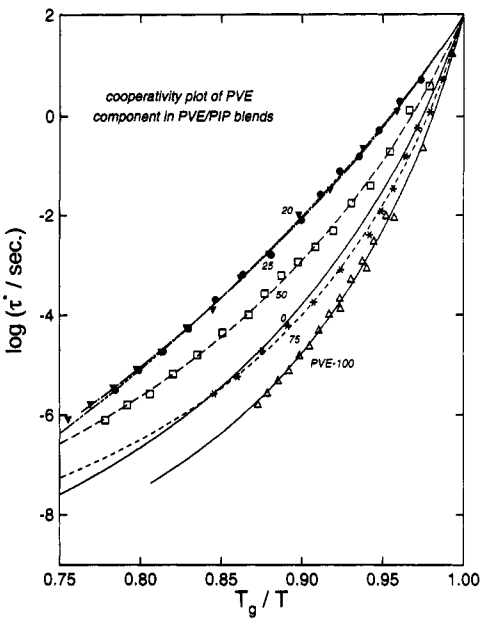

Figure 13. Cooperativity plot for the PVE component in PVE/PIP blends. The PVE content is as indicated. T_g appearing in the label of the x-axis stands for the glass temperature, T_{gPVE-x}, of the PVE component in the PVE-x blend.

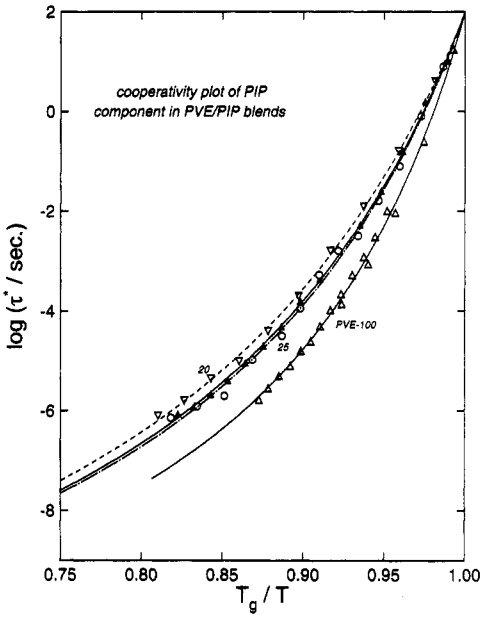

Figure 14. Cooperativity plot for the PIP component in PVE/PIP blends. The PVE content is as indicated. The solid triangles represent data for neat PIP. T_g appearing in the label of the x-axis stands for T_{gPIP} of the PIP component in the PVE-x blend.

because of the presence of conductivity loss on the low frequency side and the contribution from the PIP component on the high frequency side. Only a rough estimate is possible. Such an estimate indicates that the distribution of relaxation times of the PVE in PVE-20 has a full width at half-height (fwhh) equal to approximately two decades. Such a small fwhh corresponds to a small $\tilde{n}_{PVE}$ in PVE-20, which corroborates with its cooperation plot's drastically reduced steepness.[22-26]

(v) Cooperativity plots of log τ_{PIP}^* versus T_{gPIP}/T for the PIP component from dielectric loss data of pure PIP, PVE-15, PVE-20, and PVE-25 are shown in Figure 14. Within experimental error, there is no change in the steepness of the plot in blends with PVE content up to 25%, consistent with the fact that PIP molecules are still the major component. An estimate of the dielectric loss

spectrum for the PIP component alone in PVE-20 and PVE-25 (Figures 7 and 8) shows its width to be only slightly broader than that of pure PIP. This indicates that $\bar{n}_{PIP}$ in these blends is not too different from the coupling parameter of pure PIP, which explains why there is no change in the steepness of its cooperativity plot. The dynamic mechanical loss data of PVE-25 (Figure 4) has a fwhh of about 2.3 decades which is close to that of pure PIP. Recalling the fact that the mechanical loss in this blend is mainly associated with the PIP component, the mechanical data in Figure 4 corroborate the conclusions from dielectric loss data, i.e., the interpretation given above for $\bar{n}_{PIP}$ and the explanation of why there is little change in the steepness of the cooperativity plot of PVE-20 and PVE-25 as compared with that of PIP.

The situation changes on further addition of PVE. The fwhh of the mechanical loss peak of PVE-50 is now over 3 decades, indicating increases of both $\bar{n}_{PIP}$ and the steepness of the cooperativity plot compared with those of PVE-20 and PVE-25. Unfortunately, the narrow frequency window of mechanical measurements and the large uncertainty involved in locating the peak position at low temperatures (see error bars for the mechanical data of PVE-50 in Figure 9) make the cooperativity plot for PVE-50 less useful. For this reason it is not included in Figure 14. These trends expected for the dynamics of PIP in PVE/PIP have been observed by dielectric measurements of blends of PS with PVME.[9,10] In the PS/PVME blends the PVME plays the role of the PIP in the PVE/PIP blends. The experimental data reaffirm the increase of coupling parameter and cooperativity plot steepness for PVME in the PS/PVME blends.

Dielectric measurements performed on PS/PVME blends[9,10] and on TMPC/PS blends[12] selectively observe the dynamics of PVME and TMPC component, respectively, by taking advantage of the small dipolar relaxation strength of PS. Here, in our combined dielectric and dynamic mechanical studies of the PVE/PIP blends, both components can be "resolved". It is gratifying to see that in the *same blend system* the dynamics of the PVE and PIP components behave in the same manner respectively as TMPC in TMPC/PS and as PVME in PS/PVME. The present results confirm that the conclusions[10,12] made there are very general and applicable to both components in the same blend.

(vi) Both dielectric and mechanical relaxation data for PVE-75 (Figures 11 and 12) show that the breakdown of time–temperature superposition and broadening of the loss peak for either component occur to a greater degree than with PVE-50 (Figures 10 and 5), PVE-25 (Figures 8 and 4), or PVE-20 (Figure 7). These trends have been anticipated by the coupling model interpretation of component dynamics in blends.

Conclusion

By taking advantage of the prominence of the PIP component contribution to dynamic mechanical relaxation and the PVE component in dielectric relaxation, we have been able to resolve the dynamics of both components in PVE/PIP blends. As proposed earlier,[8,10,15] not only the composition fluctuations inherent to any blend but also the intrinsically different relaxation characteristics of the components determine the behavior of the blend. The capacity for intermolecular coupling of a pure polymer (corresponding in the coupling model to the magnitude of its coupling parameter, n) is dependent on chemical structure. It determines the characteristics of the local segmental relaxation of the polymer, as we have shown in a series of papers focusing on the coupling model.[22,23,25–28] Blending with another polymer of different chemical structure will change the extent of intermolecular coupling (n), because of the replacement of segments of different chemical structure and different mobility in its environment. In addition, composition fluctuations will give rise to a distribution in the capacity of intermolecular coupling. These factors have been taken into account in a theory of blend dynamics,[8,10,15] which has provided a number of predictions concerning the dynamics in the blend and their dependence on composition. Previously, experimental measurements either could not resolve the individual dynamics or could observe only the dynamics of one component. Here, by using combined dielectric and dynamic mechanical experiments, we are able to resolve the dynamics of the components. The experimental data presented in this paper make possible detailed comparisons with the predictions of the coupling model for local segmental relaxation in blends. Good agreement between theory and experiment has been obtained.

Acknowledgment. J.C. and A.A. are supported by Iberdrola S.A., CICYT (Project MEC MAT92-0335) and Gipuzkoako Foru Aldundia. K.L.N. is supported in part by ONR Contract N0001494WX23010.

References and Notes

(1) Shears, M. S.; Williams, G. *J. Chem. Soc., Faraday Trans. 2* **1973**, *69*, 608.
(2) Wetton, R. E.; MacKnight, W. J.; Fried, J. R.; Karasz, F. E. *Macromolecules* **1978**, *11*, 158.
(3) Alexandrovich, P. S.; Karasz, F. E.; MacKnight, W. J. *J. Macromol. Sci., Phys (B)* **1980**, *17*, 501.
(4) Lau, S.; Pathak, J.; Wunderlich, B. *Macromolecules* **1982**, *15*, 1278.
(5) Lin, J.-L.; Roe, R.-J. *Polymer* **1988**, *29*, 1227.
(6) Roland, C. M.; Lee, G. F. *Rubber Chem. Technol.* **1988**, *63*, 554.
(7) Miller, J. B.; McGrath, K. J.; Roland, C. M.; Trask, C. A.; Garroway, A. N. *Macromolecules* **1990**, *23*, 4543.
(8) Roland, C. M.; Ngai, K. L. *Macromolecules* **1991**, *24*, 2261.
(9) Zetsche, A.; Kremer, F.; Jung, W.; Schulze, H. *Polymer* **1990**, *31*, 1883.
(10) Roland, C. M.; Ngai, K. L. *Macromolecules* **1992**, *25*, 363.
(11) Chung, G.-C.; Kornfield, J. A.; Smith, S., submitted to *Macromolecules*.
(12) Ngai, K. L.; Roland, C. M.; O'Reilly, J. M.; Sedita, J. S. *Macromolecules* **1992**, *25*, 3906.
(13) Rizos, A.; Fytas, G.; Alig, I.; Kremer, F.; Pakula, T. *Polymer* **1993**, *34*, 2263.
(14) Fischer, E. W.; Zetsche, A. *Polym. Prepr. (Am. Chem. Soc., Div. Polym. Chem.)* **1992**, *33*, 78.
(15) Roland, C. M.; Ngai, K. L. *J. Rheol.* **1992**, *36*, 1691.
(16) Roland, C. M. *Macromolecules*, in press.
(17) Tomlin, D. W.; Roland, C. M. *Macromolecules* **1992**, *25*, 2994.
(18) Boesse, D.; Kremer, F.; Fetters, L. J. *Macromolecules* **1990**, *23*, 1826.
(19) Adachi, K.; Kotaka, T. *Prog. Polym. Sci.* **1983**, *18*, 585.
(20) Although dielectric and dynamic mechanical relaxation frequencies at the same temperature do not necessarily coincide, the difference between them is only about one decade in pure PVE (see ref 18). The difference found herein between f_m and f_{dPVE} in PVE-50 is much larger.
(21) Colmenero, J.; Alegría, A.; Bantangelo, P. G.; Ngai, K. L.; Roland, C. M. *Macromolecules* **1994**, *27*, 407.
(22) Roland, C. M.; Ngai, K. L. *Macromolecules* **1991**, *24*, 5315.
(23) Ngai, K. L.; Roland, C. M. *Macromolecules* **1993**, *26*, 6824.
(24) Angell, C. A. In *Relaxations in Complex Systems*; Ngai, K. L., Wright, G. B., Eds.; National Technical Information Service, U.S. Department of Commerce: Springfield, VA, 1985; p 3. Angell, C. A. *J. Non-Cryst. Solids* **1991**, *131–133*, 13.
(25) Plazek, D. J.; Ngai, K. L. *Macromolecules* **1991**, *24*, 1222.
(26) Böhmer, R.; Ngai, K. L.; Angell, C. A.; Plazek, D. J. *J. Chem. Phys.* **1993**, *99*, 4201.
(27) Plazek, D. J.; Zheng, X. D.; Ngai, K. L. *Macromolecules* **1992**, *25*, 4920.
(28) Ngai, K. L.; Plazek, D. J.; Beros, C. *Macromolecules* **1993**, *26*, 1065.